Development/Plasticity/Repair

Spontaneous Calcium Spike Activity in Embryonic Spinal Neurons Is Regulated by Developmental Expression of the Na^+, K^+-ATPase β3 Subunit

Linda W. Chang[1] **and Nicholas C. Spitzer**[2]

[1]Department of Bioengineering and [2]Neurobiology Section, Division of Biological Sciences, Kavli Institute for Brain and Mind, University of California, San Diego, La Jolla, California 92093-0357

Different types and patterns of spontaneous electrical activity drive many aspects of neuronal differentiation. Neurons in the developing *Xenopus* spinal cord exhibit calcium spikes, which regulate gene transcription and neurotransmitter specification. The ionic currents necessary for spike production have been described. However, the mechanisms that generate the onset of this activity and the basis of its regulation remain unclear. Although signaling molecules appear to act on plasma membrane receptors to trigger calcium spike activity, other mechanisms for spontaneous calcium spike regulation may exist as well. Here, we analyze the developmental expression of the Na^+, K^+-ATPase β3 subunit in *Xenopus tropicalis* embryos and show that its levels are downregulated at a time during embryonic development that coincides with the onset of prominent calcium spike activity in spinal neurons. Inhibition of an earlier increase in β3 expression leads to more depolarized resting membrane potentials and results in later reduction of spike activity. This suppression of β3 levels also reduces expression of the store-operated calcium channel subunit, Orai1. These findings suggest that the Na^+, K^+-ATPase plays a role in initiating calcium spike activity and regulating calcium homeostasis.

Introduction

Calcium signals are vital for many processes during embryonic development. In the nervous system, fluctuations in intracellular calcium levels play important roles in proliferation, migration, and neuronal differentiation (Spitzer, 2006). Spontaneous calcium transients in embryonic *Xenopus laevis* spinal neurons have been shown to regulate processes including growth cone motility (Gomez and Spitzer, 1999; Gomez et al., 2001; Conklin et al., 2005; Sann et al., 2008), as well as potassium channel and neurotransmitter expression (Gu and Spitzer, 1995; Borodinsky et al., 2004).

Spontaneous calcium spikes in *X. laevis* are generated before synapse formation by long duration calcium-dependent action potentials that rely on depolarization-induced calcium influx from voltage-gated channels (Hayes and Roberts, 1973; Holliday and Spitzer, 1990; Gu et al., 1994). The ensuing calcium currents, resulting from activation of low-voltage-activated (LVA) and high-voltage-activated (HVA) calcium channels, trigger calcium-induced calcium release from intracellular stores (Holliday et al., 1991; Gu and Spitzer, 1993). During the period of calcium spiking, neurons have arrived near their mature positions in the spinal cord and are extending axons. As development progresses, increased expression of outward potassium currents gradually eliminates the calcium component of the action potential and synapses form (O'Dowd et al., 1988; Lockery and Spitzer, 1992). Although the currents necessary for driving calcium-dependent action potentials have been identified, the developmental events responsible for eliciting the period of increased spike activity remain undetermined. Temporal regulation of the Na^+, K^+-ATPase β3 subunit occurs during neurulation, suggesting a possible role for this subunit in neuronal differentiation (Good et al., 1990; Messenger and Warner, 2000). We have tested the hypothesis that appropriate developmental expression of the β3 subunit is necessary to regulate the appearance of prominent calcium spike activity.

The Na^+, K^+-ATPase is a heteromeric electrogenic pump that requires both an α and β subunit to produce a functional enzyme capable of ion transport. Four α and three β isoforms have been characterized. The larger α subunit contains the binding sites for cations, ATP, and cardiac glycosides, whereas the β subunit is important for pump assembly and plasma membrane insertion (Geering, 2001; Kaplan, 2002). Another tissue-specific subunit, γ, also modulates pump kinetics but is not crucial for α-β formation or α-β transport out of the endoplasmic reticulum (ER) (Béguin et al., 1997; Therien et al., 1997; Pu et al., 2002).

We find that *Xenopus tropicalis* neurons generate calcium spikes within a shorter developmental time window than the corresponding period of activity in *X. laevis* (Borodinsky et al., 2004). Na^+, K^+-ATPase β3 subunit expression during develop-

Received Sept. 5, 2008; revised March 6, 2009; accepted March 31, 2009.

This work was supported by National Institutes of Health (NIH) Grant R01MH074702 (N.C.S.). We thank members of our laboratory for helpful discussions and technical assistance; D. Dulcis, K. Marek, and X. Nicol for comments on this manuscript; and I. Hsieh for technical support. We also acknowledge the Genomics Core at the University of California, San Diego Center for AIDS Research (Director, Dr. Christopher Woelk; NIH–National Institute of Allergy and Infectious Diseases Grant AI36214) and the San Diego Veterans Medical Research Foundation in this work.

Correspondence should be addressed to either Linda W. Chang or Nicholas C. Spitzer, Neurobiology Section, Division of Biological Sciences, University of California, San Diego, 9500 Gilman Drive, La Jolla, CA 92093-0357. E-mail: lwchang@ucsd.edu or nspitzer@ucsd.edu.

DOI:10.1523/JNEUROSCI.4264-08.2009

 0270-6474/09/297877-09$15.00/0

ment is also different between *X. tropicalis* and that reported for *X. laevis* (Messenger and Warner, 2000). A period of β3 upregulation, followed by downregulation, immediately precedes the period of highest spontaneous calcium spike activity, suggesting that β3 expression is important for triggering calcium spiking in *X. tropicalis*. The results of knocking down β3 levels support this interesting role. Regulation of neural cell fate specification genes appears unaffected by β3 reduction, but expression of the calcium store refilling channel, Orai1, is downregulated. These results indicate that developmental regulation of the Na^+, K^+-ATPase β3 subunit is necessary to promote the appearance of early electrical excitability.

Table 1. Primers for qRT-PCR

Gene	Forward (5′⟶3′)	Reverse (5′⟶3′)	Length (bp)	GenBank accession/Ensembl ID
α1	GATGACCGCTGGAATAACGA	CAGGGCAGTAGGACAGGAAG	247	BC064884
β3	CGGACTTTGCTCTGGGATAG	GGGTTTCCTTCTGGCTTCA	108	BC062517
Orai1	CAAAGCCTCAAGCCGAACT	GCAAATAGATGGACAGCAACC	153	ENSXETT00000008123
Notch1	ACTATGGCAACGAGGAGGAG	AAGCACTGGGAGGAGGATTT	214	BC133053
Olig2	TCTTCCTCCACTATGAGCGACT	CATCTGCTTCTTGTCCTTCTTG	156	ENSXETT00000053436
Olig4	GACAGAGAATGCCTCCCAGA	ATCACTTCCCGCAGACCA	151	NM_001045715, CR848409

Materials and Methods

Generation and staging of embryos. Adult *Xenopus* females were primed and injected with human chorionic gonadotropin (Sigma-Aldrich) to induce ovulation. *X. laevis* oocytes were fertilized *in vitro*, and *X. tropicalis* embryos were acquired either by natural mating or by *in vitro* fertilization. All embryos were grown at 21–23°C in 0.1× Marc's modified Ringer's solution (MMR) (1× MMR contains 100 mM NaCl, 2 mM KCl, 1 mM $MgSO_4$, 5 mM HEPES, 0.1 mM EDTA, 2 mM $CaCl_2$, pH adjusted to 7.8) and staged according to Nieuwkoop and Faber (1967).

Cell culture. Neuron-enriched cultures were prepared from the posterior neural plate of stage 15 *X. laevis* and *X. tropicalis* embryos as described previously (Gu et al., 1994), and cells were plated 1 h after initial dissection in 35 mm tissue culture-treated plastic dishes (Corning) with 2 ml of modified Ringer's solution (MR) (116 mM NaCl, 0.67 mM KCl, 1.31 mM $MgSO_4$, 2 mM $CaCl_2$, 4.6 mM Tris base, pH adjusted to 7.8). Each dish contained cells from one embryo and all cultures were grown and imaged at room temperature (21–23°C).

In vitro *calcium imaging.* Cultured cells were incubated in MR containing 1.25 μM Fluo-4 AM (Invitrogen), 0.01% Pluronic F-127 (Invitrogen), and 0.2% DMSO (Sigma-Aldrich) for 50–60 min. Cells were washed three times after incubation and imaged in MR. Fluorescence images were acquired with a Bio-Rad MRC-600 argon laser confocal microscope (Bio-Rad) and analyzed with NIH Image 1.63 (W. Rasband, National Institutes of Health, Bethesda, MD; http://rsb.info.nih.gov/nih-image/). Young cultures (3 h *in vitro*) were imaged at 0.2 Hz for 0.5 h to minimize photodamage. Neurons were allowed to grow several hours after imaging to assess health and to verify neuronal identity after axonogenesis that generates phase-dark neurites with lengths ≥1× the cell body diameter. Cultures younger than 3 h *in vitro* could not be imaged because cells had not yet adhered to the substrate, precluding loading and washout of calcium indicator. Older cultures (≥4 h *in vitro*) were imaged at 0.2 Hz for 1 h. Calcium spikes were identified by their rise time (within 5 s to peak) and amplitude (>2 SDs from the baseline noise fluorescence). Although calcium spikes can occur in bursts, spike frequency was scored as the number of spikes per hour. Neurons that were inactive during the imaging period were not analyzed.

Embryo dissections for in vivo *studies.* Stage 15–26 embryos were dissected in wells of Sylgard-coated (Dow Corning) Petri dishes containing 1 mg/ml collagenase B (Roche). Briefly, the gut and epidermis surrounding the presumptive spinal cord were cut away, the endodermal yolk layer was removed, and embryos were secured to the Sylgard-lined wells ventral side up with 0.10-mm-diameter stainless-steel Austerlitz Minutien pins (Fine Science Tools). After pinning, the myotomes and notochord were gently removed with sharp forceps, and the solution was replaced with MR.

In vivo *calcium imaging.* Presumptive spinal cords were loaded with Fluo-4 AM according to Root et al. (2008). For KCl experiments, dissected stage 15 presumptive spinal cords were exposed to osmotically balanced 25 mM KCl for 4–5 h before imaging and loaded with Fluo-4 AM during the last hour of incubation. All imaging was performed in MR. Fluorescence images were acquired with a Leica SP5 confocal microscope (Leica) and Bio-Rad MRC-600 or 1024 confocal microscopes at 21–23°C at an acquisition rate of 0.2 Hz for 0.5 h and analyzed with NIH Image. Calcium spikes were identified as described for *in vitro* imaging. The imaged field of view for each spinal cord contained 60–100 neurons. Spinal cords that did not exhibit activity and neurons that did not spike during the imaging period were excluded from analysis.

RNA isolation and cDNA synthesis. Total RNA was isolated from whole embryos ranging in development from early neurula to tailbud stages using the RNAqueous-4PCR kit (Ambion). The jelly coats and vitelline membrane of each embryo were removed with sharp forceps before RNA harvesting. RNA concentration and quality were determined by diluting samples in nuclease-free H_2O and measuring the absorbance of each sample at 260 and 280 nm. A total of 2.5 μg of total RNA was then reverse-transcribed using the SuperScript III First-Strand Synthesis System for reverse transcription (RT)-PCR (Invitrogen) with oligo-dT_{20} primers. After reverse transcription, the cDNA was diluted and stored in frozen aliquots.

Quantitative RT-PCR. Selection of primers was performed with Primer3 (http://frodo.wi.mit.edu/cgi-bin/primer3/primer3_www.cgi) and cross-dimer formation was checked with NetPrimer (Premier Biosoft International). All primers listed in Table 1 were synthesized by Allele Biotech and used at a final concentration of 200 nM each. A total of 10 ng of cDNA template were used per reaction. cDNA diluted from 11 embryos was used for the Na^+, K^+-ATPase subunit assay per stage and candidate gene studies were performed with diluted cDNA from 5 β3 MO-treated and 5 untreated embryos per stage. Results were averaged for $n \geq 3$ individual runs from separate clutches of embryos. All reactions were run in triplicate on an ABI PRISM 7900HT Sequence Detection System (Applied Biosystems) with default settings for absolute quantitation using a standard curve and *Power* SYBR Green PCR Master Mix (Applied Biosystems).

Construction of plasmid DNA standards for quantitative RT-PCR. Regions of each gene examined were amplified by RT-PCR using Platinum *Taq*DNA Polymerase High Fidelity (Invitrogen) with the same primers used for quantitative RT-PCR (qRT-PCR). RT-PCR products were electrophoresed on a 2% agarose gel and purified with the QIAquick Gel Extraction kit (QIAGEN). Fragments were subsequently cloned into pCR2.1-TOPO vectors using the TOPO TA Cloning kit (Invitrogen) and the resulting plasmids amplified and purified. Samples were diluted in triplicate and optical density readings were averaged to determine final DNA concentration. Plasmids were then sequenced to verify that correct inserts were cloned, and each unique DNA standard was serially diluted and stored in aliquots at −80°C.

Morpholino design and blastomere injections. The splice-blocking Na^+, K^+-ATPase β3 subunit lissaminated antisense morpholino oligonucleotide (β3 MO) (5′-AAATGAATGATCGGCTTTCTCACCC-3′) was directed to the first splice donor site of the β3 primary RNA sequence and synthesized by GeneTools. The preliminary genomic sequence of the β3 subunit was obtained by aligning the β3 mRNA sequence to the JGI *X. tropicalis* genome assembly (version 4.1) using the BLAST alignment search tool to determine exon–intron boundaries. Splice junctions were confirmed by amplifying intron 1 of the β3 gene with RT-PCR and sequencing the resulting product (Eton Bioscience). Primers used for intron amplification were located in exon 1 (5′-CAAGGAAGAGAACAAGGGAAGC-3′) and exon 2 (5′-GGTATTTGGGGACAGAATCATC-3′). To verify the identity of misspliced transcripts, primers pE1 (5′-AGAACAAGGGAAGCGAGCAG-3′), pI1 (5′-CAAAGCAAAGCAGACAGAGG-3′), and pE3 (5′-AAGCCCAGCAGATTTAGGAG-3′) were used. A

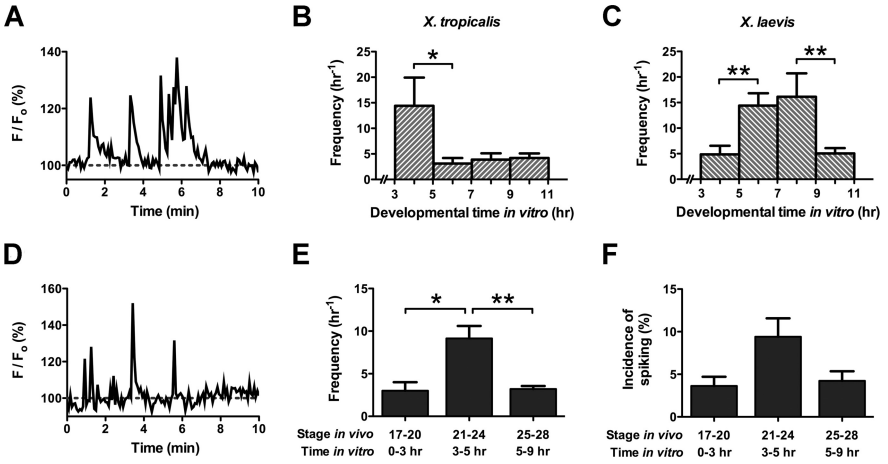

Figure 1. Embryonic amphibian spinal neurons exhibit spontaneous Ca^{2+} spike activity during growth *in vitro* and *in vivo*. ***A***, Ca^{2+} spike activity of a *X. tropicalis* neuron at 3 h in culture. Spikes are often generated in bursts. ***B***, ***C***, Distinct periods of increased spike activity occur during neuronal development in two different frog species. In *X. tropicalis* neurons *in vitro*, Ca^{2+} spike frequency is highest between 3 and 5 h of development. Ca^{2+} spike frequency of *X. laevis* neurons *in vitro* is highest between 5 and 9 h of development (*$p < 0.05$, **$p < 0.01$; $n = 9$–23 neurons/group from >5 cultures). ***D***, Ca^{2+} spike activity of a *X. tropicalis* neuron on the ventral surface of the spinal cord at stage 22. ***E***, Ca^{2+} spike activity is elevated in *X. tropicalis* neurons *in vivo* at the corresponding time of development *in vitro*. Neurons on the ventral surface of the spinal cord exhibit high frequencies of Ca^{2+} spiking between stages 21 and 24 (*$p < 0.05$, **$p < 0.01$; $n = 3$–10 embryos/stage). ***F***, The incidence of spiking on the ventral spinal cord is also high at these stages, although the variance prevents it from achieving significance. All values are means ± SEM.

standard lissaminated control morpholino (CMO) (5′-CCTCTTACCT-CAGTTACAATTTATA-3′) (GeneTools), which does not target *Xenopus* genes was used as a negative control. For imaging and electrophysiology experiments, one blastomere of a two-cell stage embryo was injected with 10–20 ng of β3 MO. For qRT-PCR, embryos were injected at the one-cell stage with 21–26 ng of β3 MO. Healthy embryos were transferred to Petri dishes containing 0.1× MMR after injections and incubated in the dark.

Electrophysiology. Intracellular recordings were made from ventral spinal neurons using sharp electrodes backfilled with 1 M potassium acetate. Stage 21/22 embryos were dissected, transferred to a Sylgard-lined recording chamber filled with MR, and pinned ventral side up at the rostral and caudal ends. Electrodes were pulled to have a resistance of 25–45 MΩ, and membrane potentials were measured *in vivo* within 1 h of dissection using an Axoclamp-2B amplifier (Molecular Devices) in bridge mode. Fresh saline was replaced every 20 min. Experiments were blinded by identifying the β3 MO-treated side by fluorescence microscopy only after measurements were made.

Statistical analysis. Statistical analyses were performed using GraphPad Prism 5 (GraphPad Software). Calcium spike frequency and incidence were analyzed with Kruskal–Wallis tests followed by Dunn's post test and Mann–Whitney *U* tests. All other data were analyzed with two-tailed paired or unpaired *t* tests unless otherwise indicated. Data are presented as means ± SEM. Results are considered significant when $p < 0.05$.

Results

Calcium spikes in *Xenopus* embryonic spinal neurons *in vitro*

Previous studies of calcium spike activity in embryonic amphibian neurons focused on neurons from the *X. laevis* spinal cord (Gu et al., 1994; Gu and Spitzer, 1995; Borodinsky et al., 2004). To determine the firing behavior of *X. tropicalis* spinal neurons, we first analyzed calcium spiking *in vitro*, and cultured neurons in 2 mM instead of 10 mM calcium medium because this more closely approximates the *in vivo* concentration of calcium ions. Neural ectoderms of *X. tropicalis* embryos were dissociated, plated, and allowed to develop in culture. Cells were loaded with the fluorescent calcium indicator dye Fluo-4 AM, and spike activity was assayed by confocal microscopy. Digitized traces of fluorescence levels in each neuron over time were analyzed and scored for spikes (Fig. 1*A*).

The average firing frequency of *X. tropicalis* neurons is highest between 3 and 5 h of growth *in vitro*. At these times, neurons spike at a rate of 14.4 ± 5.5 h^{-1} (Fig. 1*B*). During 5–7 h, the frequency of calcium spikes declines to 3.1 ± 1.1 h^{-1} and does not return to the high levels seen between 3 and 5 h at later time points (Kruskal–Wallis, $p < 0.05$, followed by Dunn's post test, $p < 0.05$). We also analyzed spike activity in *X. laevis* spinal neurons grown in 2 mM calcium culture medium for comparison with neurons from *X. tropicalis*. Before 5 h of development, the average number of spikes recorded is 4.9 ± 1.7 h^{-1}. Between 5 and 7 h, calcium spike frequency increases to 14.4 ± 2.4 h^{-1} and remains high (16.1 ± 4.6 h^{-1}) through 7–9 h of development *in vitro* (Fig. 1*C*). This developmental pattern parallels that previously described for these neurons when grown in 10 mM calcium culture medium (Gu and Spitzer, 1995). After 9 h, the number of spikes recorded decreases to 5.0 ± 1.0 h^{-1}. The mean frequencies seen between 3–5 and 9–11 h are significantly different from those seen during the 5–9 h time window (Kruskal–Wallis, $p < 0.001$, followed by Dunn's post test, $p < 0.01$). These results demonstrate that, although the average numbers of spikes recorded per hour in *X. tropicalis* and *X. laevis* neurons are comparable, the period of higher frequency calcium spiking *in vitro* appears earlier in *X. tropicalis* neurons than in *X. laevis* neurons.

Calcium spikes in *Xenopus* embryonic spinal neurons *in vivo*

The neuronal cultures consist of heterogeneous populations of cells from the spinal cord. Although neurons located on both dorsal and ventral surfaces spike *in vivo* in *X. laevis*, those positioned on the ventral surface spike at higher frequencies (Gu et al., 1994; Borodinsky et al., 2004; Root et al., 2008). To analyze the window of calcium spike activity in *X. tropicalis* neurons *in vivo*, we thus considered the likelihood that ventral neurons constitute the majority of cultured neurons seen firing calcium spikes, and imaged the intact ventral spinal cord at stages that most closely coincide with *in vitro* development (Fig. 1*D*). Stages 21–24 encompass development between 3 and 5 h *in vitro*, and stages 25–28 coincide with development between 5 and 9 h *in vitro*. Since spike analysis of cultured neurons was not possible before 3 h *in vitro*, we also examined calcium spike activity at stages 17–20, which best correspond to these early time points.

Between stages 17 and 20, spinal neurons are rarely active and few spinal cords exhibit spike activity ($n = 3$ of 13 spinal cords). Nevertheless, active neurons fire calcium spikes at an average rate of 3.0 ± 1.0 h^{-1}. The mean spike frequency increases to 9.1 ± 1.5 h^{-1} between stages 21 and 24 and falls back down to 3.2 ± 0.4 h^{-1} between stages 25 and 28 (Kruskal–Wallis, $p < 0.001$, followed by Dunn's post test, $p < 0.05$) (Fig. 1*E*). These findings indicate that, in *X. tropicalis*, spike timing *in vivo* matches spike timing *in vitro*. The incidence of spiking seen in *X. tropicalis* spinal neurons during development *in vivo* parallels the trend seen for spike frequency. Between stages 17 and 20, the percentage of

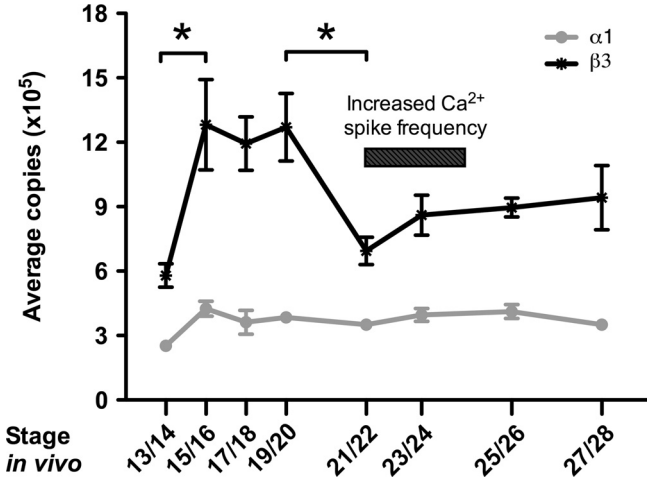

Figure 2. Temporal expression of Na^+, K^+-ATPase α1 and β3 subunits in *X. tropicalis* embryos during development. Quantitative RT-PCR shows that β3 mRNA transcript levels are significantly upregulated during development between stages 15 and 20, whereas no significant fluctuation of α1 mRNA transcript levels occurs between stages 15 and 28. β3 transcript levels are downregulated at stage 21/22, coinciding with the period of increased Ca^{2+} spiking observed both *in vivo* and *in vitro* (*$p < 0.05$). Values are means ± SEM for $n = 4$ independent experiments.

spiking neurons in active spinal cords is 3.6 ± 1.1% h^{-1}. The incidence subsequently increases to 9.4 ± 2.2% h^{-1} during stages 21–24 and declines to 4.2 ± 1.1% h^{-1} between stages 25 and 28 (Fig. 1*F*). In *X. laevis,* the patterns of calcium spiking appear to be different. The duration of calcium spike activity *in vivo* is longer in *X. laevis* than in *X. tropicalis* [compare Fig. 1*E* and Borodinsky et al. (2004), their Fig. 1*f*], and incidence and frequency trends across stages are not as well correlated (Borodinsky et al., 2004).

Developmental regulation of Na^+, K^+-ATPase subunits

Sodium pump activity is required for neuronal differentiation of *X. laevis* neurons *in vitro* (Messenger and Warner, 1979). The Na^+, K^+-ATPase in embryonic *X. laevis* is composed of α1, β1, β2, β3, and γ subunits (Good et al., 1990; Davies et al., 1996; Messenger and Warner, 2000; Eid and Brändli, 2001). Although the α1 subunit is present in a variety of structures including the neural plate (Davies et al., 1996), only β3 of the known β isoforms is expressed in the developing spinal cord, and the γ subunit is not detected (Eid and Brändli, 2001). Therefore, we assayed α1 and β3 transcript levels with qRT-PCR from the onset of neurulation through the tailbud stages of developing *X. tropicalis* embryos to determine whether developmental changes in Na^+, K^+-ATPase expression would overlap temporally with calcium spike activity.

α1 transcripts are expressed at relatively low levels at stage 13/14. An increase of ~70% occurs by stage 15/16, and these transcript levels are maintained through stage 28 (Fig. 2). Similarly, β3 levels are also relatively low at stage 13/14 and significantly increase by ~100% at stage 15/16. Unlike α1, β3 transcripts remain high through stage 19/20 and then decrease significantly at stage 21/22 to levels comparable with those observed at stage 13/14 (one-way ANOVA, $p = 0.0027$, followed by Newman–Keuls *post hoc* test, $p < 0.05$). A slight increase in β3 occurs beginning at stage 23/24 and transcripts are sustained at this level through stage 28. At all stages examined, β3 transcripts are present in higher amounts than α1 transcripts. Similar observations have been made in several developing rat tissues (Orlowski and Lingrel, 1988), rat skeletal muscle (Lavoie et al., 1997), and mammalian kidney cell lines, and may be attributed to the more rapid degradation rate of the β subunit compared with the α subunit (Mircheff et al., 1992; Lescale-Matys et al., 1993).

Knockdown of β3 subunit expression alters neuronal membrane potential

These results indicate that upregulation and later downregulation of β3 transcripts occurs during two distinct periods of development: neurulation and the appearance of calcium spike activity. The upregulation of β3 between stages 15 and 20 during neural tube formation corresponds to a previously reported hyperpolarization of the membrane potential in neural plate cells during nervous system development (Blackshaw and Warner, 1976), and the timing of β3 downregulation at stage 21/22 is closely linked to the onset of increased calcium spike activity (Fig. 1*E*,*F*). To address whether upregulation and subsequent downregulation of the sodium pump is necessary for the appearance of these calcium spikes, a splice-blocking morpholino was used to knock down β3 expression.

To confirm the efficacy of the β3 MO, multiplex RT-PCR was performed on cDNA from stage 15/16 control uninjected, CMO- and β3 MO-injected embryos using primers designed to exon 1, intron 1, and exon 3 (Fig. 3*A*). Two different sized PCR fragments were anticipated. The first corresponds to the correctly spliced wild-type β3 mRNA that produces normal β3 protein (Fig. 3*B*, top). The second corresponds to a misspliced β3 transcript that retains the first intron. This variant of β3 should cause a frameshift mutation that prematurely truncates the protein after translation of the first exon (Fig. 3*B*, bottom). RT-PCR amplifies a single band in both control and CMO-treated embryos (Fig. 3*C*), as expected for the correctly spliced β3 transcript. In β3 MO-treated embryos, a larger product corresponding to the intron-retaining transcript is amplified in addition to the wild-type fragment. Sequencing of the amplicons confirmed the identity of the wild-type band and the aberrantly spliced β3 product. Incomplete knockdown was essential to the study since knocking out various pump subunits during development is lethal (Magyar et al., 1994; James et al., 1999; Ikeda et al., 2003, 2004; Madan et al., 2007).

Embryos injected with the β3 MO did not look morphologically different from control or CMO-injected embryos at the stages examined. However, β3 MO-treated embryos remained immobile and unresponsive when touched with a glass probe between late tailbud through larval stages, in contrast to controls that rapidly swam away. This paralysis was observed in >95% of embryos treated with the β3 MO but was not apparent in either control or CMO-treated embryos (data not shown).

Reducing β3 expression should decrease Na^+, K^+-ATPase activity and consequently affect the membrane potential of developing neurons. Accordingly, we measured the resting membrane potential of ventral spinal neurons in unilaterally β3 MO-treated embryos to quantify the knockdown (Fig. 3*D*). Neurons on the control side display an average membrane potential of −36.5 ± 1.6 mV. Decreasing β3 levels raises the resting potential to −19.6 ± 1.6 mV, which is significantly different from controls, demonstrating that neurons on the β3 MO-injected side have more depolarized resting membrane potentials than those on the control side (two-tailed unpaired *t* test, $p < 0.0001$).

Knockdown of β3 subunit expression reduces calcium spiking

Unilaterally β3 MO-treated spinal cords were also loaded with Fluo-4 AM between stages 17 and 24 and imaged to establish

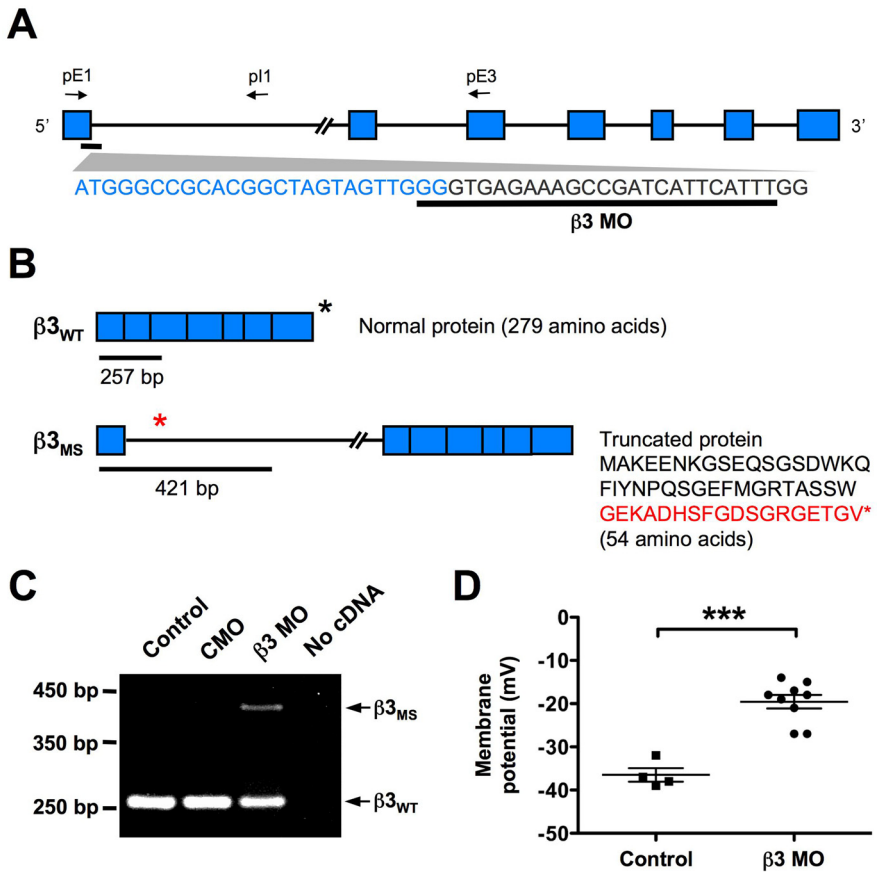

Figure 3. A splice-blocking morpholino (β3 MO) disrupts normal splicing of the Na^+, K^+-ATPase β3 subunit in *X. tropicalis* and alters the membrane potential of embryonic spinal neurons. ***A***, Schematic of β3 unspliced RNA and the β3 MO target sequence. The blue boxes indicate exons, connecting lines represent introns, and arrows show approximate locations of primers used for RT-PCR. ***B***, Predicted splicing of β3 mRNA in wild-type embryos and embryos after β3 MO treatment. Primers shown in ***A*** amplify a 257 bp fragment in wild-type β3 mRNA ($\beta3_{WT}$) (top) and a 421 bp fragment in misspliced β3 mRNA ($\beta3_{MS}$) (bottom). $\beta3_{WT}$ generates a 279 aa protein, whereas conceptual translation of the predicted $\beta3_{MS}$ produces a 54 aa protein. The last 18 aa of this truncated protein (red text) are translated from the first intron. The asterisks represent the stop codon location in each transcript. ***C***, RT-PCR of stage 15/16 β3 MO-treated embryos using primers shown in ***A*** yields predicted spliced and misspliced products schematized in ***B***. Control uninjected and CMO-treated embryos do not produce the $\beta3_{MS}$ transcript. ***D***, Intracellular recordings of stage 21/22 ventral spinal neurons from embryos injected with β3 MO in one blastomere at the two-cell stage. Neurons on the β3 MO-treated side display significantly more depolarized membrane potentials than neurons on the control side (***$p < 0.0001$). Each point represents a recording from a single neuron. The horizontal lines represent the mean ± SEM.

whether Na^+, K^+-ATPase expression plays a role in regulating calcium spike activity (Fig. 4*A*). The one-half of the spinal cord treated with the lissaminated β3 MO was identified by red fluorescence (Fig. 4*B*) and the merged image revealed that spiking neurons were predominantly located on the contralateral control side (Fig. 4*C*). Before neural tube closure (stages 17–20), 1.2 ± 0.7% of neurons spike per hour on the β3 MO-treated side, whereas 3.5 ± 1.4% of neurons spike per hour on the control side (Mann–Whitney *U* test, $p > 0.18$) (Fig. 4*D*). In contrast, the incidence of spiking neurons on the control side is 11.8 ± 1.9% h^{-1} during stages 21–24. When β3 is knocked down, the percentage of active neurons drops to 0.6 ± 0.4% h^{-1} (Mann–Whitney *U* test, $p < 0.0001$). The significant change in incidence between β3 MO-treated and untreated embryos during stages 21–24, but not 17–20, indicates that β3 expression is necessary between stages 17 and 20 for the initiation of calcium spike activity.

Spike frequencies in control and β3 MO-treated neurons also follow similar trends. During stages 17–20, neurons on the β3 MO-treated side of the spinal cord fire spikes at a rate of only 2 h^{-1}, which does not differ significantly from the control side frequency of 3.0 ± 1.0 h^{-1}. Between stages 21 and 24, β3 knockdown reduces the mean spiking rate to 3.2 ± 0.8 h^{-1}. This is significantly lower than the average spike frequency seen on the control side (14.4 ± 1.8 h^{-1}) (Mann–Whitney *U* test, $p < 0.05$) (Fig. 4*E*).

Because β3 MO treatment causes depolarization of neurons, we determined whether a similar effect on calcium spiking is produced by sustained depolarization with 25 mM KCl. Higher concentrations of KCl caused isolated spinal cords to dissociate gradually during the 4–5 h incubation period encompassing stages 15–20, precluding calcium imaging. Spike incidence and frequency were normal when KCl was not applied (12.1 ± 2.6% h^{-1}; 14.2 ± 1.6 h^{-1}; $n = 60$ neurons from six embryos), and abolished when KCl was applied and not washed out (data not shown). Prolonged application of 25 mM KCl followed by washout reduced both the incidence and frequency of spiking (6.5 ± 0.6% h^{-1}; 8.7 ± 1.1 h^{-1}; $n = 51$ neurons from eight embryos) (Fig. 5). These results indicate that the effect of chronic depolarization parallels the effect of β3 MO treatment.

Na^+, K^+-ATPase activity and gene expression

Neuronal calcium signals use calcium influx from voltage-gated channels located in the plasma membrane as well as calcium released from intracellular ER stores (Berridge, 1998); both are required to generate calcium spike activity (Holliday and Spitzer, 1990; Holliday et al., 1991; Gu et al., 1994). The mechanisms of calcium release from stores involving activity of inositol triphosphate and ryanodine receptors are well described (Berridge, 1998). In comparison, less is known about the mechanisms of store-operated calcium entry (SOCE) and store-operated calcium channels (SOCs), which replenish depleted stores. The most notable SOC is the calcium release-activated calcium (CRAC) channel. CRAC modulator 1 (Orai1) constitutes the pore-forming subunit of the CRAC channel and is activated by the ER calcium sensor STIM1 (Feske et al., 2006; Prakriya et al., 2006; Soboloff et al., 2006; Vig et al., 2006; Yeromin et al., 2006; Lewis, 2007). Although SOCs and SOCE have been studied primarily in inexcitable cells, evidence now suggests that SOCE is also present in neurons (Bouron, 2000; Emptage et al., 2001; Tobin et al., 2006).

It was recently shown that *Orai1* may have functions in the developing nervous system (Koizumi et al., 2007). To determine whether this gene is also present in embryonic *X. tropicalis* and whether knockdown of β3 affects its expression, we performed qRT-PCR to evaluate *Orai1* levels. We grouped the results according to developmentally significant events between stages 15 and 28: upregulation of β3 expression (stages 15–20), increased calcium spike activity (stages 21–24), and the period after increased calcium spike activity (stages 25–28). In wild-type em-

bryos, *Orai1* transcripts are present throughout stages 15–20 and increase ~25% during development between stages 15–20 and 21–24 (Fig. 6*A*). Transcripts then remain at this elevated level through stage 28. When β3 is knocked down, *Orai1* expression decreases concomitantly. At stages 15–20 and 21–24, transcript levels fall 25 and 35%, respectively, from levels seen in wild-type embryos. *Orai1* transcripts then increase slightly from stages 21–24 to stages 25–28, although levels are still significantly lower than those seen in wild-type embryos (two-tailed paired *t* test, $p < 0.05$).

We also investigated whether modulation of Na^+, K^+-ATPase activity affects expression of genes known to be involved in neural differentiation. Transcript levels of Notch homolog 1 (*Notch1*), oligodendrocyte transcription factor 2 (*Olig2*), and oligodendrocyte transcription factor 4 (*Olig4*) were examined in both treated and untreated embryos. These genes were chosen as controls for the β3 MO treatment. Notch signaling plays roles in cell fate determination including the maintenance of neuronal progenitors and neuronal and glial differentiation (Louvi and Artavanis-Tsakonas, 2006; Shimojo et al., 2008), whereas the *olig* genes are basic helix-loop-helix transcription factors thought to be important for oligodendrocyte development. *Olig2* is located on the ventral surface of the spinal cord and is required to maintain motoneuron and oligodendrocyte precursors (Kessaris et al., 2001; Zhou et al., 2001; Lu et al., 2002; Zhou and Anderson, 2002; Rowitch, 2004). The less well characterized *Olig4* is localized to the dorsal spinal cord and to date has only been found in the genomes of fish and amphibians (Bronchain et al., 2007). Nonetheless, its expression seems to be necessary for the differentiation of interneurons and astrocytes (Filippi et al., 2005; Bronchain et al., 2007).

A small decrease in the number of *Notch1* transcripts occurs between stages 21 and 24 in wild-type embryos. However, this is not significantly different from the levels seen at stages 15–20 or stages 25–28. Likewise, no noticeable change in transcript levels is apparent between stages 15 and 28 among wild-type and β3 MO-treated embryos (Fig. 6*B*). The differences in *olig* gene expression among wild-type and β3 MO-treated embryos are also insignificant. *Olig2* transcript levels remain stable throughout the stages examined and *Olig4* levels steadily decline during development (Fig. 6*C*,*D*). Thus, whereas *Orai1* expression is markedly decreased by β3 knockdown, *Notch1*, *Olig2*, and *Olig4* expression are not affected.

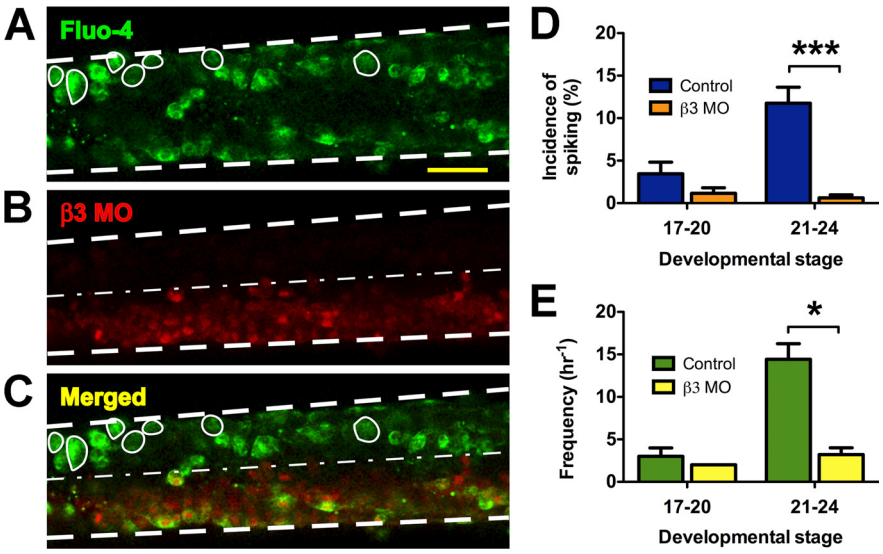

Figure 4. Ca^{2+} imaging of ventral spinal neurons from β3 MO-treated embryos. ***A***, A spinal cord is shown loaded with Fluo-4 AM pseudocolored green. Spiking neurons are circled; the margins of the spinal cord are indicated by bold dashed lines. Scale bar, 50 μm. ***B***, The one-half of the spinal cord treated with β3 MO is labeled in red. The thin dashed line indicates the midline. ***C***, A merged image of ***A*** and ***B*** shows that spiking neurons are more prevalent on the control side of the embryo. ***D***, The incidence of spiking neurons is significantly reduced in β3 MO-treated neurons compared with controls between stages 21 and 24 but not different between stages 17 and 20 (***$p < 0.0001$). ***E***, β3 knockdown does not affect the frequency of spikes observed at stages 17–20. Between stages 21 and 24, frequency is reduced from control levels (*$p < 0.05$). Values are means ± SEM for $n = 4$–17 embryos/stage.

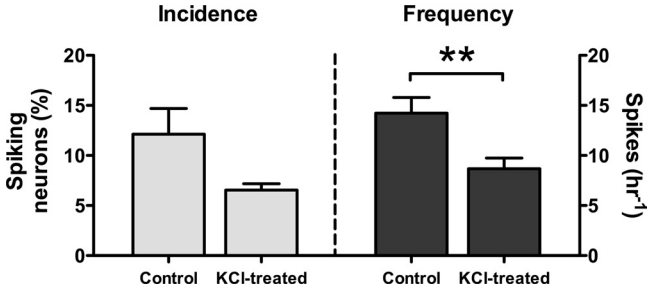

Figure 5. Ca^{2+} imaging of ventral spinal neurons in KCl-treated embryos. The incidence of calcium spiking in presumptive spinal cords dissected at stage 15 and treated with 25 mM KCl is lower than the incidence in controls. The frequency of calcium spiking in these KCl-treated spinal cords is also less than the frequency in controls (**$p < 0.01$). Values are means ± SEM for $n = 6$–8 embryos/condition.

Discussion

Determining the level of sodium pump expression during early neuronal development is critical to understanding its role in driving spontaneous calcium spiking. The Na^+, K^+-ATPase directly affects the ionic gradients that maintain resting membrane potentials, which influence the activation of voltage-gated channels. In embryonic *X. tropicalis*, neuronal calcium spikes occur within a window of development after neural tube closure but before the formation of fully functional neuronal networks. Expression of the Na^+, K^+-ATPase β3 subunit is upregulated during neurulation and downregulated at the time calcium spikes appear. Suppressing expression of β3 shifts membrane potentials to more depolarized values and inhibits the appearance of spontaneous calcium spikes. Depolarization of the membrane potential with KCl produces a similar effect. These results support a model that requires activation of the Na^+, K^+-ATPase to initiate the cascade of events necessary for spike production (Fig. 7).

β3 regulation and calcium channel activity

Developmentally regulated β3 expression is required for the appearance of calcium spikes, linking Na^+, K^+-ATPase activity with calcium signaling. However, the mechanism by which increased β3 expression leads to activation of calcium channels necessary for spike production is unknown. We suggest that the activity of the Na^+, K^+-ATPase before neural tube formation removes sustained inactivation of LVA calcium channels, by hyperpolarizing the membrane potential. Additionally, it may facilitate channel insertion into the membrane.

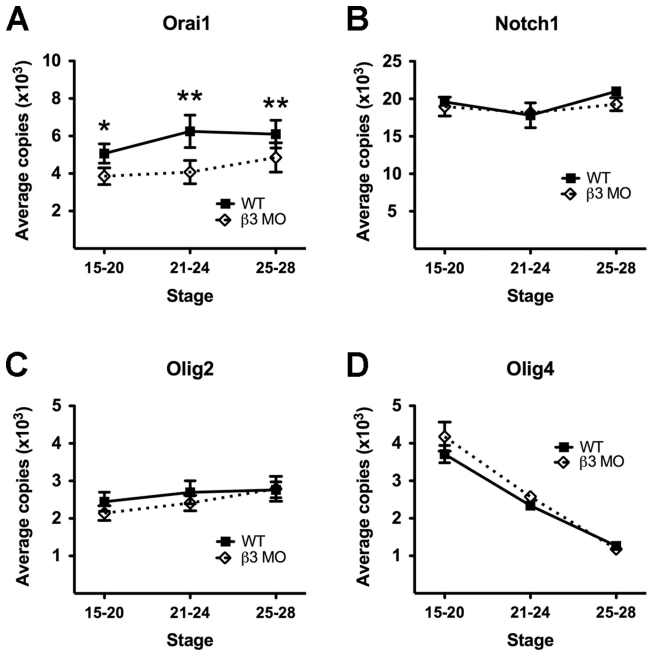

Figure 6. Decreased sodium pump expression reduces *Orai1* gene expression during embryonic development. ***A***, When β3 levels are knocked down, transcript levels of *Orai1* are significantly reduced between stages 15 and 28 ($*p < 0.05$, $**p < 0.01$). Decreased β3 levels do not cause significant changes in *Notch1* (***B***), *Olig2* (***C***), and *Olig4* (***D***) transcripts at the stages examined. All values are means ± SEM for $n \geq 3$ independent experiments.

LVA T-type calcium currents appear early in neuronal development before HVA N- and L-type calcium currents in several neuronal populations, including mammalian hippocampal neurons (Yaari et al., 1987), chick sensory dorsal root ganglia (Gottmann et al., 1988), and chick motoneurons (McCobb et al., 1989). LVA currents are also activated at much lower thresholds than HVA currents and are present in embryonic *X. laevis* spinal neurons (Desarmenien et al., 1993; Gu and Spitzer, 1993). The importance of LVA current for calcium spike activity has been demonstrated in these neurons *in vitro*. Blocking this current eliminates calcium spike activity as effectively as inhibiting HVA current, indicating a role for LVA current in activating HVA currents (Gu and Spitzer, 1993). The average resting membrane potential obtained when β3 expression levels are decreased is substantially more positive than the voltage at which neuronal T current is completely inactivated in cultured *X. laevis* spinal neurons, suggesting that the failure of spike generation could be attributable to inactivation of LVA current. This would then prevent HVA activation and calcium-induced calcium release. It is also possible that failure to activate LVA current prevents HVA channel expression. Blocking T-type calcium channel activity early in development inhibits subsequent HVA calcium channel expression in NG108-15 neuroblastoma-glioma cells that are able to recapitulate well characterized neuronal properties (Chemin et al., 2002). However, whether this occurs in *Xenopus* spinal neurons has yet to be determined.

In addition, we find that knocking down β3 expression decreases the transcription of *Orai1*, which encodes a pore-forming subunit of a store-operated calcium channel. This suggests that there may be a decreased number of SOCs present in the plasma membrane, leading to a reduction in store refilling. Because spike amplitudes range in size and are mostly dependent on intracellular calcium stores (Holliday et al., 1991), the reduction in calcium levels will lead to an elimination of small spikes and a consequent reduction in overall spike frequency. The expression levels of other components regulating calcium spiking may change as well. These include ion channels that can raise the threshold for action potential initiation, further reducing the frequency and appearance of calcium spikes.

β3 regulation and neuronal differentiation

Differentiation of cultured embryonic *X. laevis* neurons is inhibited when sodium pump activity is blocked during neurulation by strophanthidin, a cardiac glycoside that reversibly binds to the Na^+, K^+-ATPase (Messenger and Warner, 1979). To determine whether the lack of calcium spike activity could be attributed to failure of neurons to differentiate from precursors or to respecification of neurons to other cell types, we examined the expression levels of three genes involved in regulating neuronal and glial differentiation: *Notch1*, *Olig2*, and *Olig4*. No significant changes in any of these transcripts were observed as a result of β3 knockdown.

Downregulation of *Notch* transcripts has been reported after strophanthidin treatment during neurulation (Messenger and Warner, 2000), which may have resulted either from species variation or from the severity of the knockdown strategy used. The morpholino concentrations used here may have inhibited pump activity to a lesser extent and certainly caused far fewer abnormal phenotypes than the strophanthidin concentrations used in previous studies (Messenger and Warner, 1979; Messenger and Warner, 2000). However, our findings suggest that the β3 MO treatment was effective in reducing Na^+, K^+-ATPase expression. When β3 levels are reduced, the membrane potential of ventral neurons becomes more depolarized compared with control neurons, consistent with reduced Na^+, K^+-ATPase activity. Moreover, a paralyzed phenotype is seen with the β3 knockdown embryos, resembling that observed in animals with abnormal α subunit expression in other systems. Newborn mice lacking the α2 isoform exhibit no motor activity and die shortly after birth from lack of respiratory activity even though they have beating hearts (Moseley et al., 2003), whereas a mutation in the sole *Drosophila* α subunit causes bang-sensitive paralysis that is phenocopied in wild-type flies injected with ouabain (Schubiger et al., 1994). Our results provide a mechanistic understanding of the observation that pump activity is necessary for some aspects of development (Messenger and Warner, 1979, 2000; Breckenridge and Warner, 1982; Rowe et al., 1993), by providing a link between membrane potential and calcium spikes.

Other modes of calcium spike regulation

Recent work has shown that GABA and glutamate released at early stages of development bind to metabotropic receptors and regulate calcium spike activity in *X. laevis*. When these receptors are blocked, the incidence of spiking neurons decreases, suggesting that these neurotransmitters modulate spike activity (Root et al., 2008). In contrast, our findings identify a different mechanism regulating the onset of calcium spike activity in *X. tropicalis*. One possibility is that different neuronal populations use different mechanisms for generating calcium spikes, since blocking metabotropic receptors with pharmacological antagonists only prevents a subpopulation of neurons from spiking (Root et al., 2008). Another possibility is that neurons use different machinery to initiate the period of calcium spiking in different species or at different times during this period in both species. It would be interesting to determine whether reducing sodium pump activity alters GABA and glutamate expression in the developing spinal cord before the onset of activity, and whether the two mecha-

nisms are linked. Reducing sodium pump activity during early neuronal development could prevent calcium channel expression or activation, which would then preclude effects of neurotransmitter receptor activation on calcium spike activity. Alternatively, the intracellular signaling cascades activated by these metabotropic receptors could impact Na^+, K^+-ATPase function and provide a feedback mechanism with which to regulate calcium spiking.

Adhesive roles of β subunits

Other Na^+, K^+-ATPase β subunits have adhesive roles in addition to facilitating ion transport. The Na^+, K^+-ATPase β2 subunit functions as an adhesion molecule on murine glia, where it is involved in neuron–astrocyte adhesion and promotes neurite outgrowth in a calcium-independent manner (Antonicek et al., 1987; Gloor et al., 1990; Müller-Husmann et al., 1993). The β1 subunit also has roles in cell–cell adhesion and the formation of trophectoderm tight junctions (Shoshani et al., 2005; Vagin et al., 2006; Madan et al., 2007). This role appears to be shared among β subunit isoforms of voltage-gated sodium channels as well; their β2 subunit is able to bind to tenascins, and the β1 subunit can bind to the cell adhesion molecules Nf186, contactin, and NrCAM (neuron–glia-related cell adhesion molecule) (Srinivasan et al., 1998; McEwen and Isom, 2004). Although the adhesive functions of the Na^+, K^+-ATPase β3 subunit in the nervous system are currently unknown, it would be interesting to examine whether altering β3 expression affects cellular processes such as neuronal migration and neurite outgrowth during development.

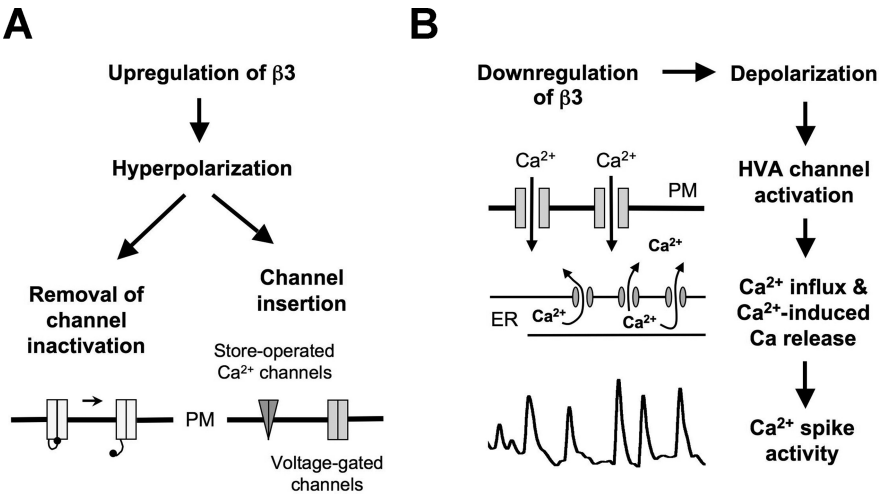

Figure 7. Model of the roles of β3 expression during neuronal development. ***A***, Upregulation of β3 hyperpolarizes neurons, allowing removal of inactivation of calcium channels and/or insertion of voltage-gated or store-operated channels into the plasma membrane (PM). ***B***, Subsequent downregulation of β3 triggers a cascade of events necessary for Ca^{2+} spike production including activation of HVA current, calcium-induced calcium release, and refilling of the ER.

References

Antonicek H, Persohn E, Schachner M (1987) Biochemical and functional characterization of a novel neuron-glia adhesion molecule that is involved in neuronal migration. J Cell Biol 104:1587–1595.

Béguin P, Wang X, Firsov D, Puoti A, Claeys D, Horisberger JD, Geering K (1997) The γ subunit is a specific component of the Na, K-ATPase and modulates its transport function. EMBO J 16:4250–4260.

Berridge MJ (1998) Neuronal calcium signalling. Neuron 21:13–26.

Blackshaw SE, Warner AE (1976) Alterations in resting membrane properties during neural plate stages of development of the nervous system. J Physiol 255:231–247.

Borodinsky LN, Root CM, Cronin JA, Sann SB, Gu X, Spitzer NC (2004) Activity-dependent homeostatic specification of transmitter expression in embryonic neurons. Nature 429:523–530.

Bouron A (2000) Activation of a capacitative Ca^{2+} entry pathway by store depletion in cultured hippocampal neurones. FEBS Lett 470:269–272.

Breckenridge LJ, Warner AE (1982) Intracellular sodium and the differentiation of amphibian embryonic neurones. J Physiol 332:393–413.

Bronchain OJ, Pollet N, Ymlahi-Ouazzani Q, Dhorne-Pollet S, Helbling JC, Lecarpentier JE, Percheron K, Wegnez M (2007) The *olig* family: phylogenetic analysis and early gene expression in *Xenopus tropicalis.* Dev Genes Evol 217:485–497.

Chemin J, Nargeot J, Lory P (2002) Neuronal T-type α1H calcium channels induce neuritogenesis and expression of high-voltage-activated calcium channels in the NG108-15 cell line. J Neurosci 22:6856–6862.

Conklin MW, Lin MS, Spitzer NC (2005) Local calcium transients contribute to disappearance of pFAK, focal complex removal and deadhesion of neuronal growth cones and fibroblasts. Dev Biol 287:201–212.

Davies CS, Messenger NJ, Craig R, Warner AE (1996) Primary sequence and developmental expression pattern of mRNAs and protein for an α1 subunit of the sodium pump cloned from the neural plate of *Xenopus laevis.* Dev Biol 174:431–447.

Desarmenien MG, Clendening B, Spitzer NC (1993) *In vivo* development of voltage-dependent ionic currents in embryonic *Xenopus* spinal neurons. J Neurosci 13:2575–2581.

Eid SR, Brändli AW (2001) *Xenopus* Na, K-ATPase: primary sequence of the β2 subunit and *in situ* localization of α1, β1, and γ expression during pronephric kidney development. Differentiation 68:115–125.

Emptage NJ, Reid CA, Fine A (2001) Calcium stores in hippocampal synaptic boutons mediate short-term plasticity, store-operated Ca^{2+} entry, and spontaneous transmitter release. Neuron 29:197–208.

Feske S, Gwack Y, Prakriya M, Srikanth S, Puppel SH, Tanasa B, Hogan PG, Lewis RS, Daly M, Rao A (2006) A mutation in Orai1 causes immune deficiency by abrogating CRAC channel function. Nature 441:179–185.

Filippi A, Tiso N, Deflorian G, Zecchin E, Bortolussi M, Argenton F (2005) The basic helix-loop-helix *olig3* establishes the neural plate boundary of the trunk and is necessary for development of the dorsal spinal cord. Proc Natl Acad Sci U S A 102:4377–4382.

Geering K (2001) The functional role of β subunits in oligomeric P-type ATPases. J Bioenerg Biomembr 33:425–438.

Gloor S, Antonicek H, Sweadner KJ, Pagliusi S, Frank R, Moos M, Schachner M (1990) The adhesion molecule on glia (AMOG) is a homologue of the β subunit of the Na, K-ATPase. J Cell Biol 110:165–174.

Gomez TM, Spitzer NC (1999) *In vivo* regulation of axon extension and pathfinding by growth-cone calcium transients. Nature 397:350–355.

Gomez TM, Robles E, Poo M, Spitzer NC (2001) Filopodial calcium transients promote substrate-dependent growth cone turning. Science 291:1983–1987.

Good PJ, Richter K, Dawid IB (1990) A nervous system-specific isotype of the β subunit of the Na^+, K^+-ATPase expressed during early development of *Xenopus laevis.* Proc Natl Acad Sci U S A 87:9088–9092.

Gottmann K, Dietzel ID, Lux HD, Huck S, Rohrer H (1988) Development of inward currents in chick sensory and autonomic neuronal precursor cells in culture. J Neurosci 8:3722–3732.

Gu X, Spitzer NC (1993) Low-threshold Ca^{2+} current and its role in spontaneous elevations of intracellular Ca^{2+} in developing *Xenopus* neurons. J Neurosci 13:4936–4948.

Gu X, Spitzer NC (1995) Distinct aspects of neuronal differentiation encoded by frequency of spontaneous Ca^{2+} transients. Nature 375:784–787.

Gu X, Olson EC, Spitzer NC (1994) Spontaneous neuronal calcium spikes and waves during early differentiation. J Neurosci 14:6325–6335.

Hayes BP, Roberts A (1973) Synaptic junction development in the spinal cord of an amphibian embryo: an electron microscope study. Z Zellforsch Mikrosk Anat 137:251–269.

Holliday J, Spitzer NC (1990) Spontaneous calcium influx and its roles in differentiation of spinal neurons in culture. Dev Biol 141:13–23.

Holliday J, Adams RJ, Sejnowski TJ, Spitzer NC (1991) Calcium-induced release of calcium regulates differentiation of cultured spinal neurons. Neuron 7:787–796.

Ikeda K, Onaka T, Yamakado M, Nakai J, Ishikawa TO, Taketo MM, Kawakami K (2003) Degeneration of the amygdala/piriform cortex and enhanced fear/anxiety behaviors in sodium pump α2 subunit (Atp1a2)-deficient mice. J Neurosci 23:4667–4676.

Ikeda K, Onimaru H, Yamada J, Inoue K, Ueno S, Onaka T, Toyoda H, Arata A, Ishikawa TO, Taketo MM, Fukuda A, Kawakami K (2004) Malfunction of respiratory-related neuronal activity in Na^+, K^+-ATPase α2 subunit-deficient mice is attributable to abnormal Cl^- homeostasis in brainstem neurons. J Neurosci 24:10693–10701.

James PF, Grupp IL, Grupp G, Woo AL, Askew GR, Croyle ML, Walsh RA, Lingrel JB (1999) Identification of a specific role for the Na, K-ATPase α2 isoform as a regulator of calcium in the heart. Mol Cell 3:555–563.

Kaplan JH (2002) Biochemistry of Na,K-ATPase. Annu Rev Biochem 71:511–535.

Kessaris N, Pringle N, Richardson WD (2001) Ventral neurogenesis and the neuron-glial switch. Neuron 31:677–680.

Koizumi K, Higashida H, Yoo S, Islam MS, Ivanov AI, Guo V, Pozzi P, Yu SH, Rovescalli AC, Tang D, Nirenberg M (2007) RNA interference screen to identify genes required for *Drosophila* embryonic nervous system development. Proc Natl Acad Sci U S A 104:5626–5631.

Lavoie L, Levenson R, Martin-Vasallo P, Klip A (1997) The molar ratios of α and β subunits of the Na^+-K^+-ATPase differ in distinct subcellular membranes from rat skeletal muscle. Biochemistry 36:7726–7732.

Lescale-Matys L, Putnam DS, McDonough AA (1993) Na^+-K^+-ATPase α1- and β1-subunit degradation: evidence for multiple subunit specific rates. Am J Physiol 264:C583–C590.

Lewis RS (2007) The molecular choreography of a store-operated calcium channel. Nature 446:284–287.

Lockery SR, Spitzer NC (1992) Reconstruction of action potential development from whole-cell currents of differentiating spinal neurons. J Neurosci 12:2268–2287.

Louvi A, Artavanis-Tsakonas S (2006) Notch signalling in vertebrate neural development. Nat Rev Neurosci 7:93–102.

Lu QR, Sun T, Zhu Z, Ma N, Garcia M, Stiles CD, Rowitch DH (2002) Common developmental requirement for *olig* function indicates a motor neuron/oligodentrocyte connection. Cell 109:75–86.

Madan P, Rose K, Watson AJ (2007) Na/K-ATPase β1 subunit expression is required for blastocyst formation and normal assembly of trophectoderm tight junction-associated proteins. J Biol Chem 282:12127–12134.

Magyar JP, Bartsch U, Wang ZQ, Howells N, Aguzzi A, Wagner EF, Schachner M (1994) Degeneration of neural cells in the central nervous system of mice deficient in the gene for the adhesion molecule on glia, the β2 subunit of murine Na, K-ATPase. J Cell Biol 127:835–845.

McCobb DP, Best PM, Beam KG (1989) Development alters the expression of calcium currents in chick limb motoneurons. Neuron 2:1633–1643.

McEwen DP, Isom LL (2004) Heterophilic interactions of sodium channel β1 subunits with axonal and glial cell adhesion molecules. J Biol Chem 279:52744–52752.

Messenger EA, Warner AE (1979) The function of the sodium pump during differentiation of amphibian embryonic neurones. J Physiol 292:85–105.

Messenger NJ, Warner AE (2000) Primary neuronal differentiation in *Xenopus* embryos is linked to the β3 subunit of the sodium pump. Dev Biol 220:168–182.

Mircheff AK, Bowen JW, Yiu SC, McDonough AA (1992) Synthesis and translocation of Na^+-K^+-ATPase α-and β-subunits to plasma membrane in MDCK cells. Am J Physiol 262:C470–C483.

Moseley AE, Lieske SP, Wetzel RK, James PF, He S, Shelly DA, Paul RJ, Boivin GP, Witte DP, Ramirez JM, Sweadner KJ, Lingrel JB (2003) The Na,K-ATPase α2 isoform is expressed in neurons, and its absence disrupts neuronal activity in newborn mice. J Biol Chem 278:5317–5324.

Müller-Husmann G, Gloor S, Schachner M (1993) Functional characterization of β isoforms of murine Na,K-ATPase. J Biol Chem 268:26260–26267.

Nieuwkoop PD, Faber J (1967) Normal table of *Xenopus laevis* (Daudin), Ed 2. Amsterdam: North Holland.

O'Dowd DK, Ribera AB, Spitzer NC (1988) Development of voltage-dependent calcium, sodium and potassium currents in *Xenopus* spinal neurons. J Neurosci 8:792–805.

Orlowski J, Lingrel JB (1988) Tissue-specific and developmental regulation of rat Na,K-ATPase catalytic α isoform and β subunit mRNAs. J Biol Chem 263:10436–10442.

Prakriya M, Feske S, Gwack Y, Srikanth S, Rao A, Hogan PG (2006) Orai1 is an essential pore subunit of the CRAC channel. Nature 443:230–233.

Pu HX, Scanzano R, Blostein R (2002) Distinct regulatory effects of the Na,K-ATPase γ subunit. J Biol Chem 277:20270–20276.

Root CM, Velázquez-Ulloa NA, Monsalve GC, Minakova E, Spitzer NC (2008) Embryonically expressed GABA and glutamate drive electrical activity regulating neurotransmitter specification. J Neurosci 28:4777–4784.

Rowe SJ, Messenger NJ, Warner AE (1993) The role of noradrenaline in the differentiation of amphibian embryonic neurons. Development 119:1343–1357.

Rowitch DH (2004) Glial specification in the vertebrate neural tube. Nat Rev Neurosci 5:409–419.

Sann SB, Xu L, Nishimune H, Sanes JR, Spitzer NC (2008) Neurite outgrowth and *in vivo* sensory innervation mediated by a $Ca_v2.2$-laminin β2 stop signal. J Neurosci 28:2366–2374.

Schubiger M, Feng Y, Fambrough DM, Palka J (1994) A mutation of the *Drosophila* sodium pump α subunit gene results in bang-sensitive paralysis. Neuron 12:373–381.

Shimojo H, Ohtsuka T, Kageyama R (2008) Oscillations in Notch signaling regulate maintenance of neural progenitors. Neuron 58:52–64.

Shoshani L, Contreras RG, Roldán ML, Moreno J, Lázaro A, Matter K, Cereijido M (2005) The polarized expression of Na^+,K^+-ATPase in epithelia depends on the association between β-subunits located in neighboring cells. Mol Bio Cell 16:1071–1081.

Soboloff J, Spassova MA, Tang XD, Hewavitharana T, Xu W, Gill DL (2006) Orai1 and STIM reconstitute store-operated calcium channel function. J Biol Chem 281:20661–20665.

Spitzer NC (2006) Electrical activity in early neuronal development. Nature 444:707–712.

Srinivasan J, Schachner M, Catterall WA (1998) Interaction of voltage-gated sodium channels with the extracellular matrix molecules tenascin-C and tenascin-R. Proc Natl Acad Sci U S A 95:15753–15757.

Therien AG, Goldshleger R, Karlish SJ, Blostein R (1997) Tissue-specific distribution and modulatory role of the γ subunit of the Na,K-ATPase. J Biol Chem 272:32628–32634.

Tobin V, Gouty LA, Moos FC, Desarménien MG (2006) A store-operated current (SOC) mediates oxytocin autocontrol in the developing rat hypothalamus. Eur J Neurosci 24:400–404.

Vagin O, Tokhtaeva E, Sachs G (2006) The role of the β1 subunit of the Na,K-ATPase and its glycosylation in cell-cell adhesion. J Biol Chem 281:39573–39587.

Vig M, Peinelt C, Beck A, Koomoa DL, Rabah D, Koblan-Huberson M, Kraft S, Turner H, Fleig A, Penner R, Kinet JP (2006) CRACM1 is a plasma membrane protein essential for store-operated Ca^{2+} entry. Science 312:1220–1223.

Yaari Y, Hamon B, Lux HD (1987) Development of two types of calcium channels in cultured mammalian hippocampal neurons. Science 235:680–682.

Yeromin AV, Zhang SL, Jiang W, Yu Y, Safrina O, Cahalan MD (2006) Molecular identification of the CRAC channel by altered ion selectivity in a mutant of Orai. Nature 443:226–229.

Zhou Q, Anderson DJ (2002) The bHLH transcription factors OLIG2 and OLIG1 couple neuronal and glial subtype specification. Cell 109:61–73.

Zhou Q, Choi G, Anderson DJ (2001) The bHLH transcription factor Olig2 promotes oligodendrocyte differentiation in collaboration with Nkx2.2. Neuron 31:791–807.